and piezoelectric constants of Rochelle salt," *Phys. Rev.*, vol. 55, pp. 775–789, Apr. 1939.
[7] T. M. Reeder and D. K. Winslow, "Characteristics of microwave acoustic transducers for volume wave excitation," *IEEE Trans. Microwave Theory Tech.*, vol. MTT-17, pp. 927–941, Nov. 1969.
[8] R. Krimholtz, D. A. Leedom, and G. L. Matthaei, "New equivalent circuits for elementary piezoelectric transducers," *Electron. Lett.*, vol. 6, pp. 398–399, June 1970.
[9] A. A. Oliner, H. L. Bertoni, and R. C. M. Li, "A microwave network formalism for acoustic waves in isotropic media," *Proc. IEEE*, vol. 60, pp. 1503–1512, Dec. 1972.
[10] A. A. Oliner, R. C. M. Li, and H. L. Bertoni, "Catalog of equivalent networks for planar interfaces," *Proc. IEEE*, vol. 60, pp. 1513–1518, Dec. 1972.
[11] "Standards on Piezoelectric Crystals, 1949," *Proc. IRE*, vol. 37, pp. 1378–1395, Dec. 1949 (IEEE Standard No. 176).
[12] a) S. A. Basri, "A method for the dynamic determination of the elastic, dielectric, and piezoelectric constants of quartz," *National Bureau of Standards Monograph 9*, U.S. Dep. Commerce, June 1960, 22 pp. b) N. F. Foster, G. A. Coquin, G. A. Rozgonyi, and F. A. Vannatta, "Cadmium sulphide and zinc oxide thin-film transducers," *IEEE Trans. Sonics Ultrason.*, vol. SU-15, pp. 28–41, Jan. 1968.
[13] a) L. B. Felsen and N. Marcuvitz, "Modal analysis and synthesis of electromagnetic fields," Contract AF-19(604)-890, Rep. R-446-55 (a) and (b), Polytechnic Inst. Brooklyn, N.Y., Feb. 1956, 40 pp. (AD93662). b) W. L. Weeks, *Electromagnetic Theory for Engineering Applications*. New York: Wiley, 1964.
[14] H. J. Carlin and A. B. Giordano, *Network Theory: An Introduction to Reciprocal and Nonreciprocal Circuits*. Englewood Cliffs, N.J.: Prentice-Hall, 1964, sec. 3.16, pp. 190–207.
[15] E. K. Sittig, "Transmission parameters of thickness-driven piezoelectric transducers arranged in multilayer configurations," *IEEE Trans. Sonics Ultrason.*, vol. SU-14, pp. 167–174, Oct. 1967.
[16] E. A. Guillemin, *Introductory Circuit Theory*. New York: Wiley, 1953.

Design of Unapodized Surface-Wave Transducers with Spectral Weighting

GRAHAM R. NUDD, SENIOR MEMBER, IEEE, MICHAEL WALDNER, MEMBER, IEEE, AND R. L. ZIMMERMAN, MEMBER, IEEE

***Abstract*—The technique commonly employed to provide a wideband surface-wave transducer with a specific conversion loss as a function of frequency uses the linear frequency-modulation (LFM) (quadratic-phase) design. This provides the necessary dispersion, and apodization is then employed to obtain the required conversion loss. In some applications the apodization presents complications in that the beam generated has nonuniform width, and diffraction and phase-front problems can result. An alternate technique is described that relies on varying the number of effective transducer elements as a function of frequency to provide the conversion-loss variation. As examples of this technique, a flat bandpass filter for a nonlinear convolver and a very large fractional-bandwidth transducer (with spectral weighting to provide sidelobe control) for a memory application are described.**

I. Introduction

In many applications of surface-wave acoustics for signal processing it is necessary to control the insertion loss as a function of frequency across the band of the filter [1]. The conventional technique for achieving this is to build an array with a linear frequency-modulated (LFM) characteristic providing the wide bandwidth and then to apodize the elements within the array to provide the spectral weighting [2]. The apodization can cause problems because of the nonuniform beamwidth it produces and the variation in diffraction losses across the band.

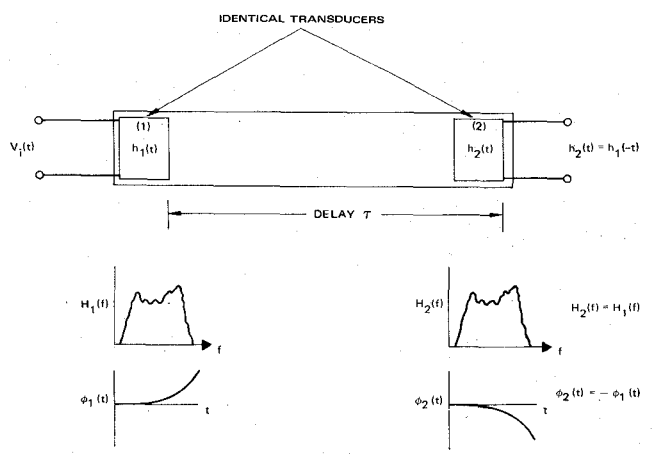

Fig. 1. Schematic of surface-wave filter.

An alternate technique which has found application in a variety of devices and avoids apodization and its associated problems, but provides a controlled insertion loss as a function of frequency, is described here. The technique relies on varying the number of elements within the array that are synchronous at any given frequency. By varying the number of effective elements $N(f)$ as a function of frequency f across the band, the insertion loss can be controlled to provide the desired spectral characteristics. This technique requires control of the finger positions to

Manuscript received January 10, 1973; revised June 17, 1973. This work was supported in part by the Wright-Patterson Air Force Base Avionics Laboratory under Contract F33615-72-C-1070, and in part by the Rome Air Development Center under Contract F30602-71-C-0196.

The authors are with Hughes Research Laboratories, Malibu, Calif. 90265.

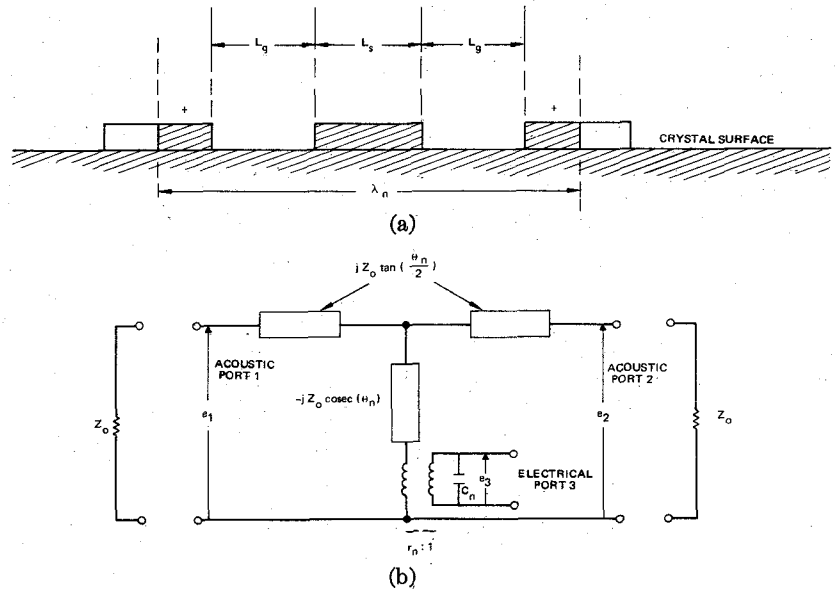

Fig. 2. (a) Transducer electrode geometry. (b) Mason equivalent circuit for single element of array.

provide the amplitude response of the filter and, hence, predetermines the phase characteristics of the individual transducer arrays. However, in many applications, including the very broad class of filters employing identical transducers for both input and output, the phase of the individual transducers is unimportant.

For instance, the output of a surface-wave acoustic filter having identical transducers (1) and (2) shown in Fig. 1 in response to an input signal $V_i(t)$ can be written as [1]

$$V_o(t+\tau) = V_i(t)*h(t)*h(-t) \tag{1}$$

where $h(t)$ is the unit impulse response of the input transducer, τ is the nondispersive delay shown in Fig. 1, and * indicates convolution. Transforming to the frequency domain we obtain

$$\begin{aligned} V_o(f)\exp[j\phi_o(f)] &= V_i(f)\exp[j\phi_i(f)] \\ &\quad \cdot H(f)\exp[j\phi_h(f)] \\ &\quad \cdot H(f)\exp[-j\phi_h(f)] \\ &\quad \cdot \exp[-j2\pi f\tau] \\ &= V_i(f)H(f)^2 \cdot \exp[j\phi_i(f)] \\ &\quad \cdot \exp(-j2\pi f\tau) \end{aligned} \tag{2}$$

where the notation that $V_0(t)$ transforms to $V_0(f)\cdot \exp[j\phi_o(f)]$, etc., is used. Hence the output signal $V_0(f)\exp[j\phi_o(f)]$ is seen to be independent of the phase of the transducers $\phi_h(f)$.

The concepts of the design of such transducers and their application to two devices, the nonlinear convolver [3] and the digital acoustic memory [4], are described below.

II. Transducer Design Techniques

Consider a transducer array consisting of N elements of the form shown in Fig. 2(a). The response of the array can be analyzed by techniques analogous to those developed by Smith *et al.* [5], where each element of the array is described by the Mason equivalent circuit [6], as illustrated in Fig. 2(b). The transformer coupling ratio r_n [7] is given by

$$r_n = (-1)^n(2f_nC_nk^2Z_0)^{1/2}\frac{K(q_n)}{K(q_n')} \tag{3}$$

where

- k electromechanical coupling constant;
- C_n static electrode capacitance of the section;
- Z_0 acoustic-wave impedance;
- f_n synchronous frequency of the element;
- L_g transducer gap dimension;
- L_s transducer electrode width;
- $q_n = \sin(\pi L_s/2(L_s+L_g))$;
- $q_n' = \cos(\pi L_s/2(L_s+L_g))$;

and K is the Jacobian complete elliptic integral of the first kind. The transit angle θ_n of the section is given by $\theta_n = (\pi/2)(f/f_n)$. In terms of the parameters of this circuit, the ratio between an applied voltage e_3 at port 3 and the equivalent voltage e_1 of the acoustic signal generated at port 1 can be written as

$$\frac{e_1}{e_3} = jr_n\sin(\theta_n)\exp(-j\theta_n). \tag{4}$$

Also, the transfer function

$$\begin{aligned} T_{13}(f) &= 2\left(\frac{G_1}{G_3}\right)^{1/2}\frac{e_1}{e_3} \\ &= j2\left(\frac{G_1}{G_3}\right)^{1/2} r_n\sin(\theta_n)\exp(-j\theta_n) \end{aligned} \tag{5}$$

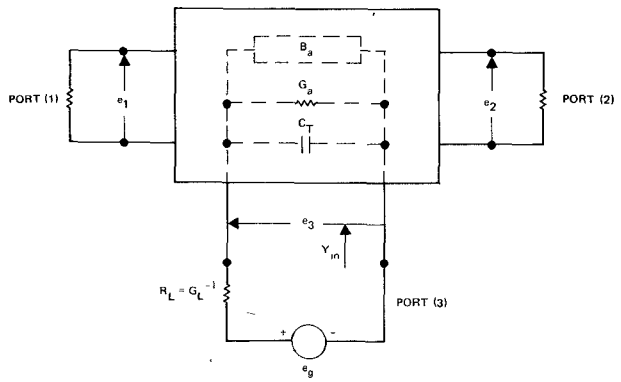

Fig. 3. Schematic of external circuit configuration.

can be defined so that the conversion loss L_{13} from electrical port 3 to acoustic port 1 is given by

$$L_{13} = | T_{13}(f) |^{-2}.$$

With reference to Fig. 3, the insertion loss (IL) between an external electrical generator e_g and the acoustic ports can be written as

$$\text{IL} = \left| \frac{2}{(Z_0 G_L)^{1/2}} \frac{e_1}{e_g} \right|^{-2} \tag{6}$$

where $e_g = e_3(G_L + Y_{\text{in}})/G_L$, or

$$\text{IL} = \left| \frac{2}{(Z_0 G_L)^{1/2}(1 + Y_{\text{in}}/G_L)} r_n \sin\left(\frac{\pi f}{2f_n}\right) \right|^{-2}. \tag{7}$$

For the entire array the response can be found by cascading the equivalent circuits for the individual sections. For this the electrical ports are connected in parallel and the equivalent acoustic terminals are summed with the appropriate phase shifts $\exp(-j\omega t_n)$, where t_n is the delay to the center of the nth section. Thus the IL and the transfer function ($T_{1g}(f)$) for the entire array can be written

$$\text{IL} = \left| \frac{2}{(Z_0 G_L)^{1/2}} \sum_{n=1}^{N} \frac{r_n}{(1 + Y_{\text{in}} R_L)} \sin\left(\frac{\pi f}{2 f_n}\right) \cdot \exp(-j\omega t_n) \right|^{-2} \tag{8}$$

and

$$T_{1g}(f) = \frac{2}{(Z_0 G_L)^{1/2}} \sum_{n=1}^{N} \frac{r_n \sin(\pi f/2f_n) \cdot \exp(-j\omega t_n)}{(1 + Y_{\text{in}} R_L)} \tag{9}$$

where $R_L = G_L^{-1}$ and $\omega = 2\pi f$. Again from the equivalent circuit of Fig. 2(b), Y_{in} can be calculated as

$$Y_{\text{in}} \simeq \hat{G}_a \sin^2(\theta_n/2) + j\hat{B}_a \sin(\theta_n) + j\omega C_T \tag{10}$$

where $\hat{G}_a = 4k^2 f_n C_n$ is the equivalent acoustic conductance at synchronism, $\hat{B}_a = 2k^2 f_n C_n$ is the equivalent acoustic susceptance at synchronism, and C_T is the static capacitance of the full array. Furthermore, for transducers with constant electrode width-to-gap ratio, $q_n = q_n' = (2)^{-1/2}$, and hence

$$\frac{K(q_n)}{K(q_n')} = 1.$$

Therefore, the capacitance of each section C_n is a constant (C_0). Hence, on low-coupling materials where the approximation $Y_{\text{in}} \simeq j\omega C_T$ can be made,

$$T_{1g}(f) \simeq \left(\frac{8k^2}{G_L}\right)^{1/2} \frac{C_0^{1/2}}{[1 + (\omega C_T R_L)^2]^{1/2}} \sum_{n=1}^{N} f_n^{1/2} \cdot \sin\left(\frac{\pi f}{2f_n}\right) \exp(-j\phi_n) \tag{11}$$

where

$$\phi_n = 2\pi f t_n + \tan^{-1}(\omega C_T R_L). \tag{12}$$

The approximate equations (11) and (12) are found to be accurate to within a few percent for most transducers of interest and hence can be used extensively in the design phase to define the finger locations and apertures.

For a two-terminal transducer with unit impulse response $h(t) \cdot \exp(-j\phi(t))$, the finger locations correspond to phases of $n\pi$, and the phase at each finger location t_n can be expressed as

$$n\pi = \phi(t_n) + \tan^{-1}(\omega C_T R_L). \tag{13}$$

For the LFM case, $h(t) = 1$ for $0 < t < T$ and zero elsewhere, and

$$\phi(t) = 2\pi[(f_0 - B/2)t + Bt^2/2T] \tag{14}$$

where B is the filter bandwidth. Substitution of this in (13) gives

$$n\pi = 2\pi\left(f_L + \frac{B}{2T} t_n\right) t_n + \tan^{-1}\left[2\pi\left(f_L + \frac{B}{2T} t_n\right) C_T R_L\right] \tag{15a}$$

where $f_L = f_0 - B/2$. Also, to first order

$$\tan^{-1}[2\pi(f_L + (B/2T)t_n) C_T R_L] \simeq \tan^{-1}(2\pi f_L C_T R_L) + \frac{\pi B C_T R_L t_n}{2T[1 + (2\pi f_L C_T R_L)^2]}$$

which substituted into (15a) results in the equation defining the finger locations for correct phase match given below

$$t_n^2 + \frac{2T}{B}\left[f_L + \frac{C_T R_L B}{2T[1 + (2\pi f_L C_T R_L)^2]}\right] t_n - \frac{2T}{B}\left[\frac{n}{2} - \frac{\tan^{-1}(2\pi f_L C_T R_L)}{2\pi}\right] = 0. \tag{15b}$$

An approximate expression for the transfer function $T_{1g}(f)$ for a constant aperture array with finger locations defined

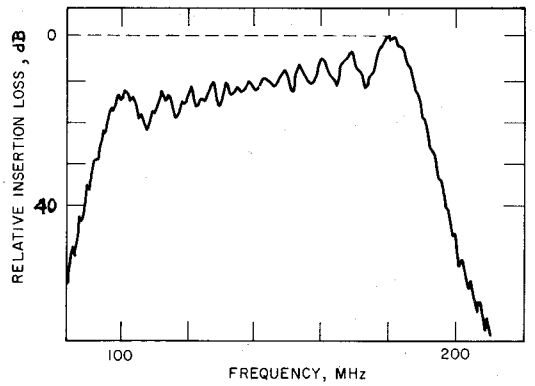

Fig. 4. Insertion loss against frequency for unapodized LFM array.

by (15b) can be found by substitution in (11) and (12), i.e.,

$$T_{1g}(f) \simeq 4f^{3/2}\left(\frac{k^2C_T}{Bf_0G_L(1+(\omega C_T R_L)^2)}\right)^{1/2} \tag{16}$$

where $C_T = f_0C_0DT$ is the total capacitance of the array. The calculated insertion loss as a function of frequency of an array with 120 fingers and a bandwidth of 70 MHz centered at 150 MHz, for example, is shown in Fig. 4. The form of the apodization required to flatten the response across the band can be derived from (8) and (16) as

$$W_n \simeq \text{const}\left(\frac{f_0}{f_n}\right)^3[1+(2\pi f_n C_T R_L)^2] \tag{17}$$

where W_n is the aperture of the nth section. The form of the array with this apodization and cosine weighting to reduce the Fresnel passband ripple is shown in Fig. 5.

The technique to produce a flat-band response, for example, and avoid the use of apodization is to vary the number of elements that are synchronous in any given frequency band. Thus, instead of starting with the phase-defining equation (13), the amplitude problem is solved. The design technique can be understood by considering the characteristics of the equation defining the overall transducer response as a function of frequency [(11)].

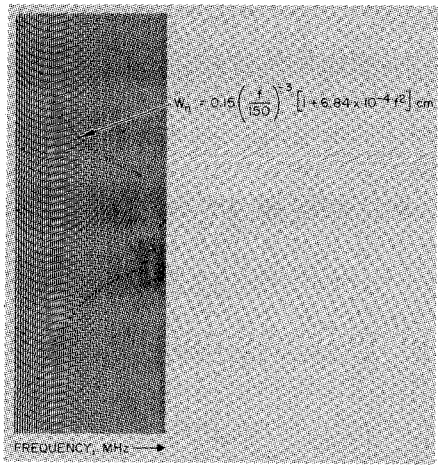

Fig. 5. Apodization required to flatten and smooth the passband of LFM array.

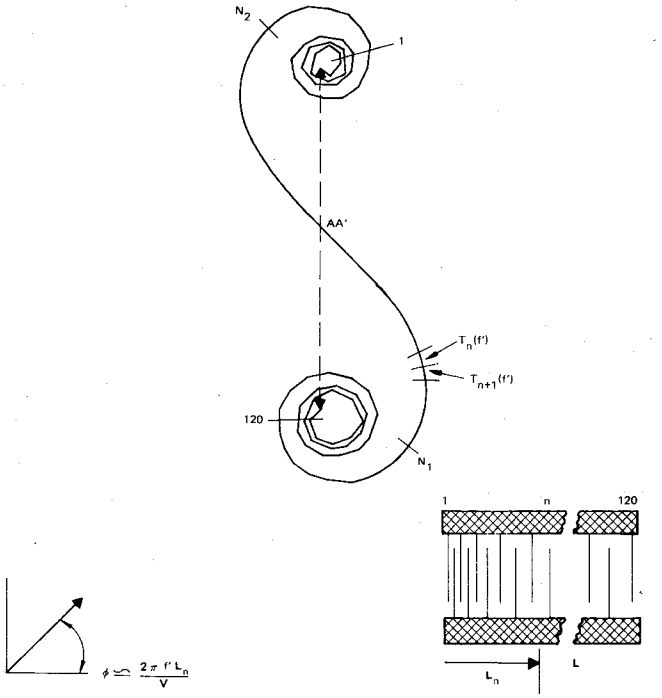

Fig. 6. Vectorial representation of $T_{1g}(f)$ [(11)] for 120-finger unapodized array.

Each term of the summation in (11) (from 1 to 120 for an array with 120 electrodes) is plotted in Fig. 6 (for a fixed frequency f') on a polar plot as a function of angle $\phi = 2\pi f' t_n$. The response of the full array $T(f')$ is then given by the vector AA' joining the ends of the summation $T_1(f')$ and $T_{120}(f')$. From Fig. 6 it can be seen that only those electrodes (N_1 to N_2) in a narrow band which are near synchronism contribute effectively to the response. The principal contribution of electrodes outside this range is to the Fresnel ripple. Hence we can write

$$T_{1g}(f) = \sum_{n=1}^{120} T_n(f) \tag{18}$$

$$T_{1g}(f) = \sum_{n=N_1}^{N_2} T_n(f) + \tilde{T}(f) \tag{19}$$

where $\tilde{T}(f)$ is a term representing the passband ripple. Furthermore, with cosine-type apodization at the ends of the array this ripple can be reduced to any desired limit, and the response can be written as

$$T_{1g}(f) \simeq T_0(f)$$

where

$$T_0(f) = 2\left(\frac{2k^2}{G_L}\right)^{1/2}\frac{C_0^{1/2}}{(1+(\omega C_T R_L)^2)^{1/2}} \cdot \sum_{N_1}^{N_2} f_n^{1/2}\sin\left(\frac{\pi f}{2f_n}\right)\exp[-j\phi_n] \tag{20}$$

and $N_2 - N_1 = N(f)$, the effective number of electrodes at frequency f. It is convenient to define $N(f)$ further so that

$$\phi_{N_2} - \phi_{N_1} = N(f)\pi + \pi \tag{21}$$

so that the phase rotation between the ends of the synchronous band is π rad.

For cases where $\omega C_T R_L \ll 1$ it can be shown [8] that

$$T_0(f) \simeq \text{const}\, N(f) f^{1/2}. \tag{22}$$

Hence for the particular case of flat-band response,

$$N(f) \propto f^{-1/2}. \tag{23}$$

An expression for the effective number of electrodes $N(f)$ in terms of the differential delay $(t_{N_2} - t_{N_1})$ can be obtained by substitution of (12) in (21), i.e.,

$$N(f) = 2f(t_{N_2} - t_{N_1}) - 1. \tag{24}$$

Furthermore, if the phase difference $\{\phi(t_{N_2}) - \phi(t_{N_1})\}$ across the active band is expressed in a Taylor series as

$$N(f)\pi \simeq 2\pi f(t_{N_2} - t_{N_1}) + \pi \frac{df}{dt}(t_{N_2} - t_{N_1})^2 \tag{25}$$

neglecting third-order terms and above, (24) yields

$$\frac{df}{dt} = -(t_{N_2} - t_{N_1})^{-2}. \tag{26}$$

Substitution of (22) and (24) in (26) yields

$$\frac{df}{dt} = -\left[\frac{2f}{1 + (\text{const})^{-1} T_0(f) f^{-1/2}}\right]^2. \tag{27}$$

For $N(f) \gg 1$, which is the case for most transducers of interest

$$\frac{df}{dt} = -\frac{4\,(\text{const})^2 f^3}{T_0(f)^2}. \tag{28}$$

Integration of (27) or (28) yields the phase characteristics required of the transducer, i.e.,

$$\phi(t) = 2\pi \iint \frac{df}{dt}\, dt\, dt \tag{29}$$

from which the delay t_n to the nth electrode can be calculated so that

$$\phi(t_n) - \phi(t_{n-1}) = \pi. \tag{30}$$

In general, it is convenient to find the finger locations x_n for a particular spectral response $H(f) = |T_0(f)|^2$ by iterative computer solution of (26)–(28) consistent with the total capacitance and aperture required of the array. However, as an illustration of this solution the important case of flat passband response is calculated. In this case $T_0(f)$ is a constant which, for convenience of calculation, is normalized to unity. The design constant referred to in (22) is then calculated in terms of the bandwidth B, total number of electrodes in the array N_T, and the upper and lower frequencies f_h and f_L of the passband. The solution of (28) for $T_0(f) = 1$ can be obtained in closed form as

$$f = \frac{(\text{const})^{-1}}{2\sqrt{2}}\, t^{-1/2} \tag{31}$$

[where const again refers to the design constant of (22)]. From this the phase characteristics of the array can be calculated from (29) as

$$\phi(t_n) = \sqrt{2}\pi\, (\text{const})^{-1}\, t_n^{1/2} + \phi_o \tag{32}$$

where ϕ_o is a constant depending on the phase reference. Furthermore, for the full array

$$\phi(t_{N_T}) - \phi(t_1) = N_T \pi \tag{33}$$

$$= \sqrt{2}\pi\, (\text{const})^{-1} [t_{N_T}^{1/2} - t_1^{1/2}] \tag{34}$$

which, after substitution in (31), can be written in terms of the frequency extremes (f_L and f_h) of the passband as

$$N_T \pi = \frac{\pi}{2}\, (\text{const})^{-2} [f_L^{-1} - f_h^{-1}]. \tag{35}$$

This yields a value for the design constant [of (22)] in terms of the design parameters as

$$\text{const} = \left(\frac{B}{2N_T f_h f_L}\right)^{1/2}. \tag{36}$$

Finally, using (30) and (32), the differential delay to each electrode can be expressed as

$$t_n = \frac{n^2 B}{4N_T f_h f_L} \tag{37}$$

and hence the position x_n of each electrode in the array can be determined by the conventional method [5] from a knowledge of the loaded and unloaded acoustic velocities. Examples of such designs for the particular cases of a flat-band response and a weighted array with 120-percent fractional bandwidth are given below.

III. Experimental Results

A. *Unapodized Flat-Band Response*

A transducer was designed, using the techniques described in Section II, and incorporated into a nonlinear convolver [9] requiring a flat passband of 75 MHz centered at 150 MHz. The form of the conventional LFM array for this is illustrated in Fig. 5. The rather coarse apodization (approximately 4:1) required to flatten the band introduces complications in this implementation. First, to couple effectively to the low frequencies, the aperture of the output coupler must be at least equal to the longest electrode in the array (0.15 cm). At the high-frequency end of the band the beam fills approximately 25 percent of the coupler; thus 75 percent of the coupler width serves only to add parasitic capacitance and reduce the coupling efficiency.

The "unapodized" bandpass transducer with 120 electrodes is shown in Fig. 7(a). At each end of the array 12 electrodes were apodized to reduce the Fresnel ripple. The calculated insertion loss of the array using the three-port network analysis given in Section II is shown in Fig. 7(b). The variation in conversion loss across the band is ap-

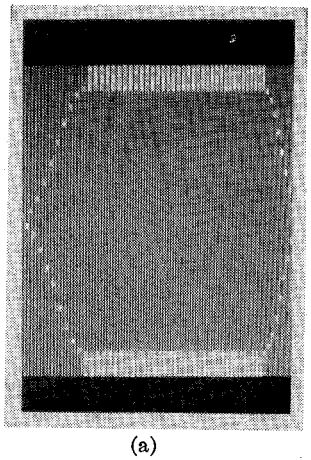

(a)

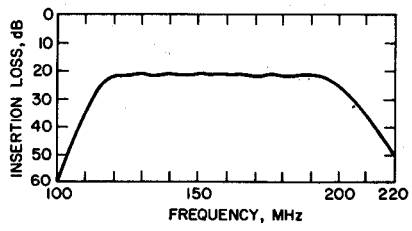

(b)

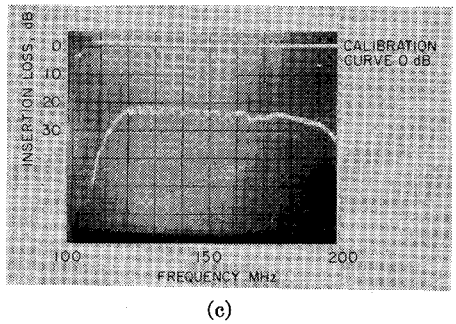

(c)

Fig. 7. (a) Unapodized array for flat bandpass characteristics. (b) Calculated insertion loss. (c) Measured insertion loss.

proximately 2 dB, which agrees well with the measured insertion loss shown in Fig. 7(c).

For an unapodized LFM array the number of effective elements $N(f)$ increases as a function of frequency as $(2DTf^2/B)^{1/2}$, where DT is the transit time of the array. This leads to an insertion loss which increases as $(2DTf^3/B)^{-2}$, giving a variation of approximately 12 dB across the band.

B. Large Fractional Bandwidth Unapodized Array with Spectral Weighting

A further application of this design technique was in a digital acoustic memory operating at 75 MHz with 67 μs of delay [4]. To obtain the required pulse-in pulse-out characteristics for a digital memory, it is necessary to control the time-domain sidelobes associated with the central peak. One technique to achieve this is to use a pair of complementary or Golay codes [10], so that the sidelobes of one code are of opposite polarity to its complement, and hence the time-domain output of the summed response is a single central lobe. In general, this technique requires two parallel channels for a single output. Techniques have been devised to provide noninteracting codes to increase the bit density [11]. However, if the bit density is increased to one cycle of carrier per bit, (i.e., Manchester encoding), the required drive signal is bipolar and requires a three-terminal transducer, as illustrated in Fig. 8.

An alternate technique to achieve the required output signal which avoids much of the associated complexity is to employ a matched filter pair with very large fractional bandwidths. If the fractional bandwidth is less than 120 percent, the output pulse is ambiguous, consisting of a number of cycles at the center frequency within the central lobe [12]. In addition, spectral weighting must be incorporated to reduce interference between adjacent bits. Signal analysis indicates that the optimum output, (i.e., the Ricker [13] waveform with zero energy at adjacent bit locations) would result from a matched filter pair with the amplitude-against-frequency characteristics shown in Fig. 9. As shown, the frequency characteristic was required to be controlled over a band from approximately 35 to 140 MHz. To make the transducer input impedance compatible with the high-speed logic required to regenerate the bits, the capacitance of the array was limited to 20 pF, equivalent to an array with an aperture of 0.15 cm and 70 fingers.

An array with 70 electrodes as shown in Fig. 10(a) was designed and fabricated, and cosine-type weighting on only three electrodes at each end was used to limit the passband Fresnel ripple. (To a large extent the time-domain output was unaffected by ripples within the band,

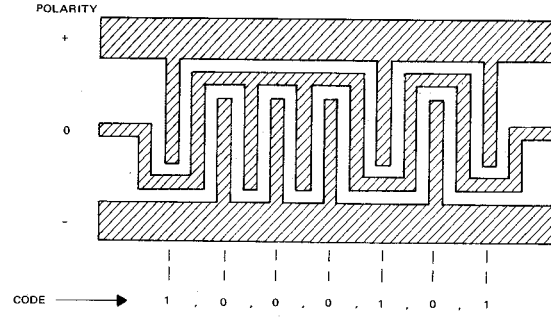

Fig. 8. Transducer required for Manchester-encoded Golay codes.

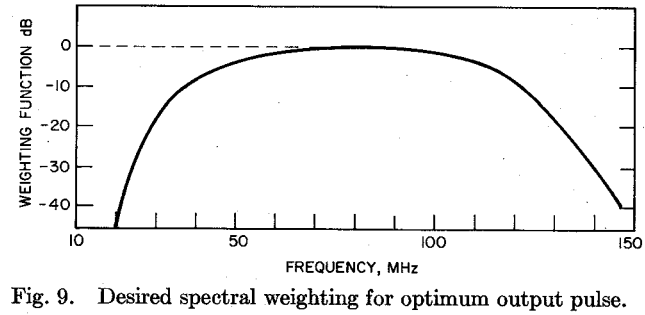

Fig. 9. Desired spectral weighting for optimum output pulse.

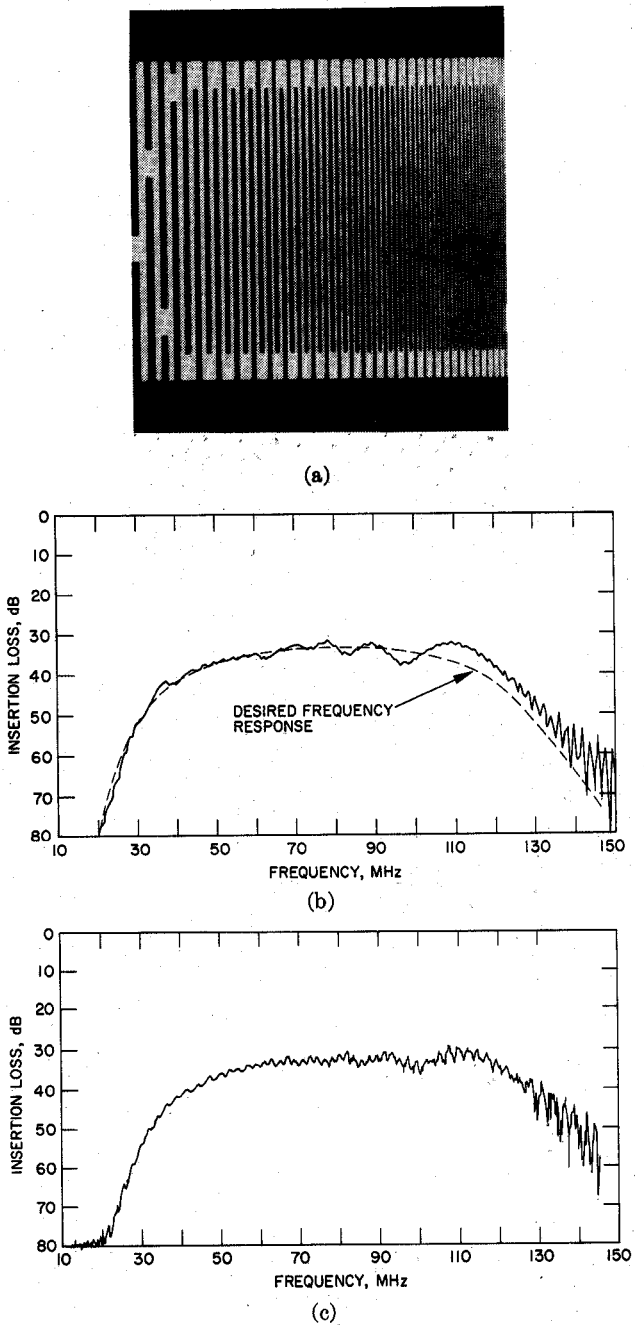

Fig. 10. (a) Form of unapodized transducer (DT = 0.5 μs). (b) Calculated insertion loss. (c) Measured insertion loss.

and hence in this application no effort was made to reduce them below 4 dB.) The calculated insertion loss versus frequency of the full array shown in Fig. 10(b) and the measured results in Fig. 10(c) can be seen to be in excellent agreement. Because of the very wide fractional bandwidth, interference from the fifth harmonic can be seen at frequencies above 125 MHz. The electrode width-to-gap ratio used in the array was unity, which has been shown [14] to effectively suppress the third harmonic but produce higher order harmonics. The coherence of these higher harmonics produces interference with the fundamental of periodicity DT. However, most of the fifth-harmonic interference in this case was beyond the spectral content of the input pulse and hence produced little degradation

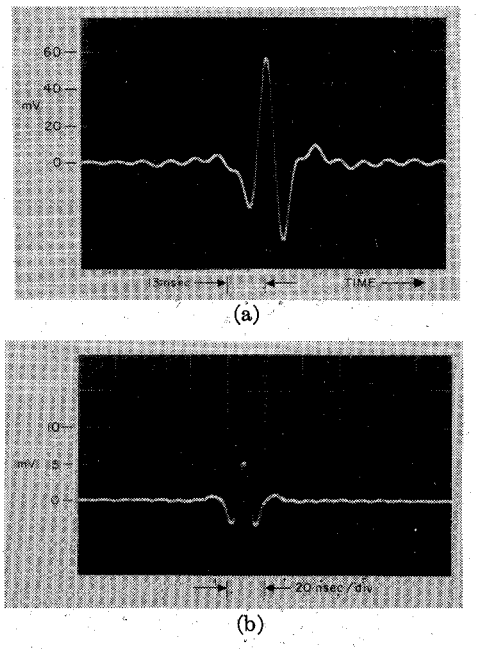

Fig. 11. (a) Output from unapodized matched filter pair. (Graticule corresponds to adjacent bit locations.) (b) Output from hybrid YZ $LiNbO_3$/ST-quartz/YZ $LiNbO_3$ 65-μs delay line. (Input pulse 5 V peak to peak.)

of the time-domain output. The output shown in Fig. 11(a) is from a 5-μs delay line on YZ $LiNbO_3$ and can be seen to be in excellent agreement with the desired Ricker output. Also, the sidelobes are such that the pulse crosses zero at all adjacent bit locations, indicating that there is no pulse-to-pulse interference, and hence the correct spectral weighting has been accomplished. The time-domain output of a single channel of the memory in its final form in response to a 5-V peak-to-peak input signal is shown in Fig. 11(b). The total delay is 67 μs, and the substrate is a hybrid structure [15] of $LiNbO_3$ for good coupling and ST quartz to minimize losses and temperature effects.

IV. Conclusion

The technique described here to avoid apodization and to achieve spectral weighting avoids many of the problems of apodization, such as varying beamwidth as a function of frequency and the problems associated with diffraction. The examples described above for the nonlinear convolver and the very large fractional-bandwidth array for the memory are cases where apodization imposed severe limits on the device performance. The unapodized technique has been shown to achieve the required transducer insertion-loss characteristics while circumventing the above constraints and thereby improving the device performance. These techniques are of particular value for spectral-weighting applications where identical arrays are employed as input and output transducers. In such applications the spectral weighting introduces no phase distortions. Also of particular interest in this area are pulse compression filters where the phase characteristics (or dispersion) can be separated from the electrical to acoustic transducers, as, for example, in the Reflective Array Compression (RAC) [16] devices.

References

[1] W. D. Squire, H. J. Whitehouse, and J. M. Alsup, "Linear signal processing and ultrasonic transversal filters," *IEEE Trans. Microwave Theory Tech. (Special Issue on Microwave Acoustics)*, vol. MTT-17, pp. 1020–1040, Nov. 1969.

[2] R. H. Tancrell and M. G. Holland, "Acoustic surface wave filters," *Proc. IEEE*, vol. 59, pp. 393–409, Mar. 1971.

[3] M. Waldner, M. E. Pedinoff, and H. M. Gerard, "Broadband surface wave nonlinear convolution filters," in *Proc. 1971 IEEE Symp. Ultrasonics* (Miami Beach, Fla.), Dec. 6–8, 1971.

[4] R. L. Zimmerman, B. P. Schweitzer, and R. C. Bender, "High data rate-high bit density acoustic digital memory," in *Proc. 1972 IEEE Symp. Ultrasonics* (Boston, Mass.), Oct. 4–7, 1972, pp. 459–364.

[5] W. R. Smith, H. M. Gerard, and W. R. Jones. "Analysis and design of dispersive interdigital surface-wave transducers," *IEEE Trans. Microwave Theory Tech.*, vol. MTT-20, pp. 458–471, July 1972.

[6] W. R. Smith, H. M. Gerard, J. H. Collins, T. M. Reeder, and H. J. Shaw, "Analysis of interdigital surface wave transducers by use of an equivalent circuit model," *IEEE Trans. Microwave Theory Tech. (Special Issue on Microwave Acoustics)*, vol. MTT-17, pp. 856–864, Nov. 1969.

[7] Coquin and Tiesten, *J. Acoust. Soc. Amer.*, vol. 41, Apr. 1967.

[8] G. R. Nudd, "Technique for varying the conversion loss against frequency of a surface wave transducer without apodization," *Electron. Lett.*, vol. 8, July 1972.

[9] M. Waldner, "Application of nonlinear interactions in acoustic media to microwave signal processing devices," Rome Air Development Center, Rome, N.Y., Contract F30602-71-C-0196, Final Rep., Aug. 1972.

[10] M. Golay, "Complementary series," *IRE Trans. Inform. Theory*, vol. IT-7, pp. 82–87, Apr. 1961.

[11] B. P. Schweitzer and J. M. Speiser, "Generalized complementary code sets," in *Proc. IEEE Int. Symp. Information Theory* (Pacific Grove, Calif.), Jan. 31–Feb. 3, 1972, p. 102.

[12] A. Papoulis, *The Fourier Integral and Its Application*. New York: McGraw-Hill, 1962, ch. 7.

[13] R. B. Rice, "Inverse convolution filters," *Geophys.*, vol. 27, pp. 4–18, Feb. 1962.

[14] R. D. Weglein and G. R. Nudd, "Space-harmonic response of surface wave transducers," in *Proc. 1972 IEEE Symp. Ultrasonics* (Boston, Mass.), Oct. 4–7, 1972, pp. 346–352.

[15] M. T. Wauk and R. L. Zimmerman, "Bonded planar structures for efficient surface wave generation," in *Proc. 1972 IEEE Symp. Ultrasonics* (Boston, Mass.), Oct. 4–7, pp. 365–366.

[16] R. C. Williamson and H. I. Smith, "Large time bandwidth product surface wave pulse compressor employing reflective gratings," *Electron. Lett.*, vol. 8, 1972.

High-Permittivity Dielectrics in Waveguides and Resonators

JEAN VAN BLADEL, SENIOR MEMBER, IEEE

Abstract—**Resonators and waveguides containing a region of high dielectric constant are considered. The dielectric constant is first assumed to be infinite, but is later given a high, but finite value. Perturbation formulas are derived for the resulting shift in either the resonant frequency of the resonator or the wavenumber of the waveguide mode.**

I. Introduction

MATERIALS of high dielectric constant and low loss-factor are now available to the microwave community. Typical values of the dielectric constant are 10 for alumina substrates, 33–38 for temperature-stable ceramics containing zirconates, and 100 or more for materials such as rutile or strontium titanate [1], [2]. Consider a cavity containing a dielectric of high dielectric constant ϵ_r and a given resonant mode therein, the lowest for example (Fig. 1). The resonant wavelength is of the order of the typical dimensions L and L_d of the cavity. Now let ϵ_r increase without limit. The resonant wavelength in the dielectric remains of the order of L_d, while the resonant frequency approaches zero. Expressed more quantitatively: a) λ_{diel} approaches a value αL_d, where α is a coefficient of order one; b) the wavenumber in the dielectric approaches a limit $k = 2\pi/\lambda_{\text{diel}} = 2\pi/\alpha L_d$; and c) the wavenumber *in vacuo* approaches a value $k/n = (1/n)(2\pi/\alpha L_d)$. Here, $n = (\epsilon_r)^{1/2}$ is the index of refraction of the dielectric. It is seen that the resonant frequency, given by $\omega/c = k/n$, approaches a value

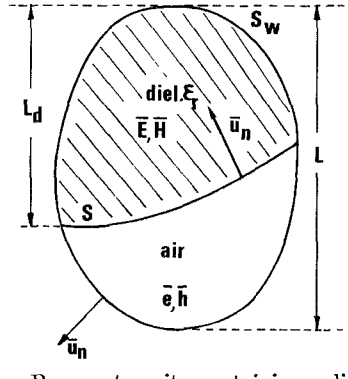

Fig. 1. Resonant cavity containing a dielectric.

$$f = \frac{c}{n\alpha L_d} = \frac{1}{2\pi}\frac{c}{n}k. \tag{1}$$

It is the purpose of this paper to calculate a second-order correction term for (1), i.e., to obtain the first two terms in a series

$$f = \frac{A}{n} + \frac{B}{n^2} + \cdots. \tag{2}$$

Manuscript received February 5, 1973; revised July 31, 1973.
The author is with the Laboratory for Electromagnetism and Acoustics, University of Ghent, Ghent, Belgium.